Spectrally Efficient Direct-Detected OFDM Transmission Incorporating a Tunable Frequency Gap and an Iterative Detection Techniques

Wei-Ren Peng, Bo Zhang, Kai-Ming Feng, Xiaoxia Wu, Alan E. Willner, *Fellow, IEEE, Fellow, OSA*, and Sien Chi, *Fellow, OSA*

***Abstract*—We analytically and experimentally demonstrate a linearly field-modulated, direct-detected virtual single-sideband orthogonal frequency-division multiplexing (VSSB-OFDM) system that employs a tunable frequency gap and an iterative detection technique. The VSSB-OFDM that uses no frequency gap, which is referred to as the gapless VSSB-OFDM, is proposed as a spectrally efficient format. Compared with the intensity-modulated SSB-OFDM, the gapless VSSB-OFDM saves half the electrical bandwidth (BW), and exhibits better receiving sensitivity and more robust tolerance against fiber chromatic dispersion (CD). Furthermore, by incorporating a tunable frequency gap between the optical carrier and the OFDM data sideband, the calculating burden of the iterative detection is greatly alleviated and the system performance can be flexibly improved within moderate iterations. The width of the optimum frequency gap is found to be $\sim$0.35 sideband BW, which is reached by trading the levels of signal–signal beat interference and the residual image beat interference. Such a gapped VSSB-OFDM system requires fewer iterations to extract the desired data from the interfered signal and exhibits greater robustness against the carrier-to-signal-power ratio (CSPR) variation, compared with the gapless VSSB-OFDM. In this paper, the analytical model of the proposed gapped VSSB-OFDM system will be addressed. In addition, we also successfully conduct a gapped VSSB-OFDM signal transmission over 1600 km of uncompensated standard single-mode fiber (SSMF) with only $\sim$3 dB optical SNR (OSNR) penalty, and obtain a significant OSNR sensitivity improvement of $\sim$8 dB, compared with the gapless VSSB-OFDM, after such a 1600-km fiber link.**

***Index Terms*—Optical-fiber communication, optical modulation, orthogonal frequency-division multiplexing (OFDM).**

I. Introduction

OPTICAL orthogonal frequency-division multiplexing (OFDM) is a seriously considered candidate for next-generation long-haul transmission because the linear impairments, such as chromatic dispersion (CD) and polarization-mode dispersion (PMD), can be electronically compensated at the receiver [1]–[4]. To date, the optical OFDM can be mainly categorized as coherent optical OFDM (CO-OFDM) and incoherent (i.e., direct-detected) optical OFDM (IO-OFDM, or DDO-OFDM). The CO-OFDM has shown its great robustness against the fiber CD and PMD using the polarization diversity technique [2], [3], [5]. When combined with polarization division multiplexing technique (PDM-OFDM), the CO-OFDM can further increase spectral efficiency (SE) and relax electronic components' bandwidth (BW) requirement at both the transmitters and receivers [2], [3]. Unfortunately, these great benefits of CO-OFDM are accompanied by high-cost installations, including narrow-linewidth laser sources, local oscillators, 90° optical hybrids, and extra signal processing accounting for the phase and frequency offset estimations. On the other hand, the DDO- OFDM can be accommodated with a low-cost DFB laser with megahertz-level linewidth [6], eliminates the local oscillators and optical hybrids, and need not estimate the phase and frequency offsets, therefore making the DDO-OFDM quite convenient to be implemented. Besides, with the self-polarization diversity technique, the direct-detected PDM-OFDM has been demonstrated for doubling SE and enhancing PMD tolerance [7]. Consequently, compromising the installation complexity and the transmission performance, the DDO-OFDM would be an alternative format for optical transmission, other than the CO-OFDM.

In DDO-OFDM, the single-sideband format (i.e., SSB-OFDM) has long been applied for long-haul transmission since it can overcome the inherent CD-induced fading problem in a double-sideband (DSB) transmission [1], [4]. In general, SSB-OFDM utilizes a frequency gap with the same size as the sideband's BW between the optical carrier and the sideband [1], [4] to prevent the signal from being interfered by the signal–signal beat interference (SSBI). Therefore, the SE in a DDO-OFDM system is only half of that in a CO-OFDM system. A recently proposed intensity- modulated SSB-OFDM (IM-SSB-OFDM) that discards this frequency gap has doubled the SE in a typical DDO-OFDM system and has been considered as a spectrally efficient format [9]–[11]. However, that technique has a design tradeoff between a better sensitivity, which requires a high optical modulation index (OMI), and robustness to fiber CD, whereas a low OMI is necessary for linear modulation [4], [10], [11]. In addition, the required transmitter's BW for generating this IM-SSB-OFDM signal is approximately twice of the output optical signal's BW because the real-valued OFDM signal is necessary for intensity modulation. Therefore, half of the transmitter BW has been wasted for carrying no effective information in transmission.

Manuscript received May 19, 2009; revised August 14, 2009. First published October 13, 2009; current version published November 25, 2009.

W.-R. Peng and S. Chi are with the Department of Photonics and the Institute of Electro-Optical Engineering, National Chiao Tung University, Hsinchu 300, Taiwan (e-mail: pwr.eo92g@nctu.edu.tw;schi@mail.nctu.edu.tw).

B. Zhang, X. Wu, and A. E. Willner are with the Department of Electrical Engineering, University of Southern California, Los Angeles, CA 90089 USA (e-mail: boz@usc.edu; xiaoxia@usc.edu; willner@usc.edu).

K.-M. Feng is with the Institute of Communications Engineering, National Tsing Hua University, Hsinchu 300, Taiwan (e-mail: kmfeng@ee.nthu.edu.tw).

Digital Object Identifier 10.1109/JLT.2009.2033304

Thus, a laudable goal to generate an SSB-OFDM signal is not only to modulate the signal more spectral efficiently, but also to preserve a high receiving sensitivity and sustain a good tolerance to fiber CD.

Recently, we have demonstrated a linearly field-modulated, direct-detected virtual SSB-OFDM (VSSB- OFDM) system that employs an RF tone at the edge of the data sideband with an iterative detection approach to reduce the SSBI [12]. Compared with the IM-SSB-OFDM, the VSSB-OFDM has relaxed the transmitter BW requirement by a factor of 2, and eliminated the tradeoff between the sensitivity and CD tolerance by electrically manipulating the power ratio between the carrier and sideband. Its operation principle and experimental results have been conceptually demonstrated in [12]. In this paper, we further provide the thorough analytical models of this VSSB-OFDM format as well as the iterative detection algorithm to have a deeper exploration and a better understanding of the proposed technique.

Although the VSSB-OFDM has lots of advantages over the IM-SSB-OFDM, its performance is still limited by some practical issues. To remove the high-power interference of SSBI, the VSSB-OFDM may introduce more computation burdens at the receiver due to the limited ability of proposed iterative algorithm. To achieve a reliable performance, at least four iterations are required [12]. Since the algorithm for each iteration will involve a fast Fourier transform (FFT) and inverse FFT (IFFT) computation, four iterations may take a long time to conduct equalization and would possibly lower the data throughput when considering a real-time receiving [17]. There are at least the following two distinct approaches to mitigate this problem: 1) develop a better-designed iterative algorithm that can remove the SSBI more efficiently, and 2) reduce the relative SSBI power, with respect to the signal power, so that the initial decisions in the iteration detection can quickly help reconstruct an accurate SSBI, and thus, increase the iteration efficiency. The first approach is beyond the scope of this paper and will not be discussed hereafter, while for the second approach, a relatively lower power of SSBI can be easily achieved by increasing the carrier-to-signal-power ratio (CSPR) via manipulating the RF amplitude. However, a larger CSPR, which assigns more optical power for carrier than the signal sideband, will yield a poor sensitivity since the optical carrier bears no information. Thus, an alternative approach to increase the processing speed of the iterative detection would be highly demanded for the future real-time VSSB-OFDM transmission.

In this paper, we present the gapped VSSB-OFDM that makes use of a tunable frequency gap to enhance the iteration efficiency by allocating part of SSBI in the gap [18]. The original idea of using the gap has been proposed in [1]and [19], in which the gap width is controlled the same as the sideband to completely avoid the SSBI. The proposed gapped VSSB format uses the similar concept to relax the burden of iterative equalizer by inserting the frequency gap. The working principle of the VSSB-OFDM, along with the previous spectrally efficient IM-SSB-OFDM, is thoroughly analyzed with their mathematical models taking all the linear impairments from the transmitter to the receiver into account. Furthermore, the proposed iterative detection for the VSSB-OFDM is specifically introduced and its working algorithm is described step by step for each iteration. The specially designed interleaved training symbol for VSSB-OFDM is then also introduced and discussed. The possible limitations of the iterative detection, such as the filtering effects resulted from the electrical and optical components, are also given and discussed. We analytically show that once the BWs of the optical filter and the electrical postdetection filter are relatively broader than the signal BW, the SSBI interference could be well estimated and cancelled from the received interfered signal. Compared with the IM-SSB-OFDM, our experimental results indicate that, in addition to its better electrical SE, the gapless VSSB-OFDM not only has $\sim$2.3 dB optical SNR (OSNR) gain but also exhibits a much improved CD tolerance. Moreover, with an optimum gap width ($\sim$0.35 sideband BW) between the carrier and the sideband, the gapped VSSB-OFDM requires fewer iterations and behaves less sensitive to CSPR, and found to outperform the gapless VSSB format by $\sim$8 dB in OSNR sensitivity after following 1600-km uncompensated standard single-mode fiber (SSMF).

This paper is constructed as follows. In Section II, the operation principles of the VSSB-OFDM, with and without the frequency gap, along with the IM-SSB-OFDM are introduced. The analytical models for the VSSB-OFDM are also given in this section. In Section III, the required signal processing and the current limitations for the iterative detection are given and discussed. The experimental setups for both gapless and gapped VSSB-OFDM systems, with four quadrature-amplitude modulation (4-QAM) at 10 Gb/s are given in Section IV; the subsequent Section V presents the experimental results and the relevant discussions. Finally, Section VI concludes this paper.

II. Principle of Operation

A. Intensity-Modulated SSB-OFDM

Fig. 1(a) schematically shows the concept of the previous IM-SSB-OFDM [9], [10]. For one OFDM symbol modulation, each set of N data QAM symbols, $d_1, d_2, \ldots, d_N$, and its conjugate counterpart, $d_1^*, d_2^*, \ldots, d_N^*$, are arranged at the positive and negative subcarriers, respectively, to achieve the Hermitian symmetry such that a real-valued electrical signal can be generated after the IFFT. This electrical signal and its Hilbert transform [13] are fed into the two arms of a quadrature-biased dual-drive Mach–Zehnder modulator (DD-MZM), thus resulting in an SSB-OFDM format. Since half the subcarriers (i.e., the negative subcarriers) are only used for the conjugates of the transmitted data, the required electrical BW (B) is double the transmitted optical BW $(2B)$. Thus, half the electrical BW, including the BW required for the DSP and the following digital-to-analog converter (DAC) in the OFDM generator, is not used for transmission and is wasted. On the other hand, the receiving sensitivity of this IM approach strongly depends on how deep the electrical signal is driven into the MZM. To measure how deep the MZM is driven, we define the OMI as $\mathrm{OMI} = (V_{\mathrm{in}})_{\mathrm{rms}}/V_\pi$, where $(V_{\mathrm{in}})_{\mathrm{rms}}$ is the root-mean-squared (rms) amplitude of the electrical input to the DD-MZM and V_π is the switching voltage of the MZM. Typically, a larger OMI value would yield a better receiving sensitivity since more signal power is transmitted along with the optical power, and *vice versa*. However, a larger OMI in MZM would result in a nonlinearly distorted signal that could not be well-equalized after the accumulated

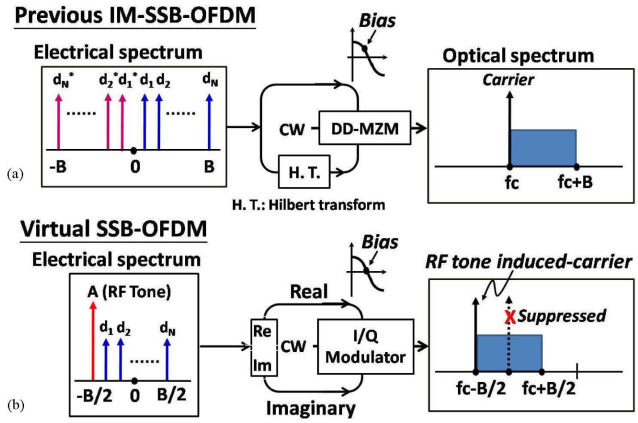

Fig. 1. Operation principles for (a) previous IM-SSB-OFDM, and (b) proposed VSSB-OFDM.

fiber CD [4]. Thus, there exists an optimum OMI value that trades the sensitivity and the transmission CD tolerance.

To achieve the generation of the IM-SSB-OFDM signal, an alternate approach is to apply an electrical mixer to up-convert the OFDM signal with the aim for relaxing the BW requirement of DAC. However, based on the signal spectrum in Fig. 1(a), an electrical mixer with an RF to IF-BW ratio of 0.5 is needed for up-converting the signal. With such an extremely low ratio, the mixer would involve extra distortions [1] into the up-converted signal and will degrade the signal performance. Thus, to exclude this inevitable penalty from the electrical mixer, we consider only the simple direct up-conversion transmitter throughout this paper.

B. Gapless VSSB-OFDM

For the gapless VSSB-OFDM, the first half of data QAM symbols, $d_1, d_2, \ldots, d_{N/2}$, and the second half of, $d_{N/2+1}, d_2, \ldots, d_N$, are allocated on the negative and positive subcarriers, respectively. One RF tone, to be located tightly at the left edge of the data subcarrier, is incorporated to assist extract the transmitted sideband with a simple photodiode. The data and the inserted RF tone are together converted to a complex-valued signal by IFFT. The real and imaginary parts of the signal are sent to the two arms of an optical I/Q modulator. With the two parallel modulators biased at the null points, the input optical carrier is suppressed and a new optical carrier induced by the inserted RF tone appears at the left edge of the signal spectrum. Because our system does not require the redundant conjugated subcarriers for the real-valued OFDM output, our system saves half the transmitter BW compared with the IM-SSB-OFDM. The required electrical BW B is equal to the transmitted optical BW B. Without using the Hilbert transform or the filtering approach, the output optical spectrum of the VSSB-OFDM signal is virtually like that of the SSB-OFDM signal. Thus, we name the proposed OFDM approach as VSSB. Note that the CSPR, defined as $\mathrm{CSPR} = |A|^2/\sum|d(k)|^2$, where A and $d(k)$ are the amplitudes of the inserted RF tone and the data on the kth subcarrier, respectively, can be optimized by controlling the relative amplitudes of the data and RF tone.

Although the gapless VSSB-OFDM method provides superior SE, which is the same as that of the CO-OFDM, the associated issue would be the more complex signal processing that needs to mitigate the SSBI on the desired signal. To reduce the complexity of the signal processing, one simple solution is the insertion of a width-tunable frequency gap between the carrier and the data sideband [18].

C. Gapped VSSB-OFDM

For linearly field-modulated, direct-detected OFDM signals, the gap width is conventionally set to be at least equal to the data sideband for completely avoiding the interference of SSBI [1], [19], [21]. However, such a gap width will not only reduce the signal's SE but will also require a higher receiver BW, thereby inevitably increasing the system's cost. Thus, with the considerations of both the SE and the iterative efficiency, a width flexible gap is needed between the optical carrier and the sideband. Fig. 2 shows the gapped VSSB-OFDM with a width-tunable frequency gap between the optical carrier and the sideband. Before we optimize the gap width, we should introduce another beat interference term, the residual image beat interference (RIBI), which results from the interaction of the limited transmitter sampling rate and the square-law photodiode. The mechanism of these image interferences are shown in Fig. 2(a). At the top of Fig. 2(a), the electrical OFDM output of the DAC circuit with a sampling rate of F_s has not only the baseband data spectrum spreading within $[-F_s/2, F_s/2]$, but also the high-frequency images that repeatedly appear in the frequency domain with a period of F_s. The reconstruction filter [15], which is used for smoothing the DAC output, following the DAC circuit can diminish these unwanted out-of-band images. Nevertheless, unless an ideal brick-wall filter is used for the reconstruction purpose, a practical filter, typically having a finite frequency roll-off around its cut-off frequency, will attenuate the in-band signal at around the Nyquist frequency, Fs/2, and will also have the out-of-band images some residual power retained, as shown at the middle of Fig. 2(a). These residual out-of-band images, including the residual carrier image (**Ai**) and the residual signal image (**Si**), would become the in-band RIBI after the photodiode, as shown at the bottom of Fig. 2(a). These residual out-of-band images would become the in-band RIBI after the photodiode, as shown at the bottom of Fig. 2(a). To mitigate the signal distortion and the level of RIBI, which includes the beat terms of $(\mathbf{A}\times\mathbf{Si})$, $(\mathbf{Ai}\times\mathbf{S})$, and $(\mathbf{S}\times\mathbf{Si})$, the signal spectrum should be kept below the Nyquist frequency by some margin that depends on the profile of reconstruction filter. Therefore, for a given Nyquist frequency (i.e., given sampling rate of DAC) and given sideband BW, a smaller gap width would allow both the signal $\mathbf{S}$, and the carrier $\mathbf{A}$, farther from the Nyquist frequency and result in a lower RIBI level. However, a smaller gap width would introduce more SSBI to the desired signal. Thus, the optimum gap width should be properly chosen to achieve the best sensitivity by trading the SSBI with the RIBI. Fig. 2(b) illustrates this tradeoff between the SSBI and RIBI. Notably, since the RIBI power is relevant to the profile of reconstruction filter, the optimum gap width will also depend on the profile of the utilized reconstruction filter. Although inserting an optimum gap in VSSB-OFDM could possibly provide some improvements in

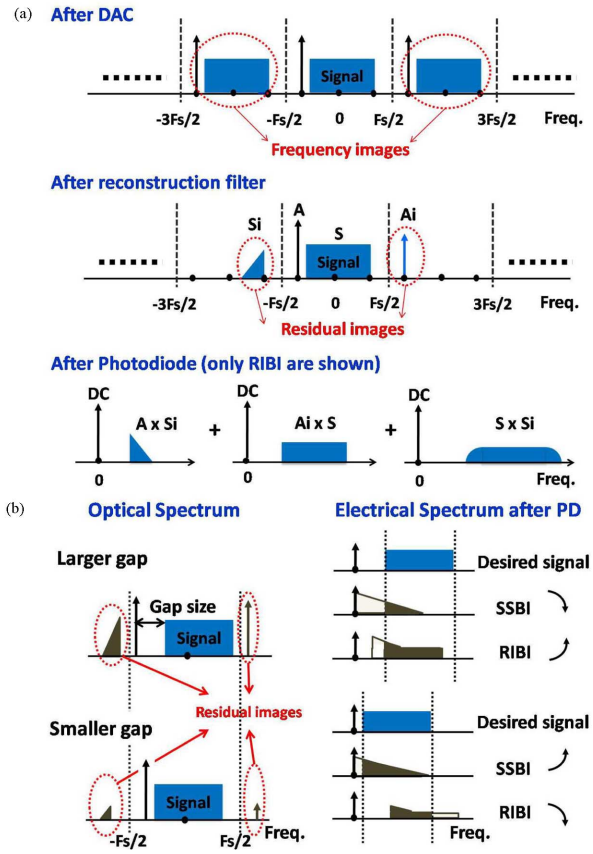

Fig. 2. (a) Origin of the RIBI in a digitally sampling system with sampling rate of Fs and (b) tradeoff of the gapped VSSB-OFDM between the SSBI ($|\mathbf{S}|^2$) and the RIBI ($\mathbf{Ai} \times \mathbf{S} + \mathbf{A} \times \mathbf{Si} + \mathbf{S} \times \mathbf{Si}$).

terms of receiving sensitivity and iteration efficiency, the price is a slight sacrifice in SE, when compared with the gapless VSSB format.

For both the gapped and gapless VSSB formats, we also define their OMI as OMI $= (V_{\text{in}})_{\text{rms}}/(2V_\pi)$. Compared to the OMI of the previous IM-SSB-OFDM system, the extra factor of two in the denominator is resulted from the doubled maximum-voltage-swing biasing at the null. In principle, the VSSB signals will have a better sensitivity with a lower OMI since it alleviates the nonlinear distortions from MZM. However, one obvious side effect of using such a small OMI value is the significant modulation loss in MZM, thus resulting in a worse output OSNR. Thus, the optimum OMI value for VSSB format could be reached by the tradeoff between a good linearity and a better OSNR of the transmitter output.

D. Theoretical Models

The mathematical models for the VSSB-OFDM are given as follows. The discrete-time electrical OFDM input, used for driving the optical modulator, can be described as

$$E(n) = Ae^{j2\pi(-N_2)n/N} + \sum_{k=N_1}^{N_2} d(k)e^{j2\pi kn/N} \tag{1}$$

where n is the discrete time index, k is the subcarrier index, A is the assigned amplitude of the RF tone at the $(-N_2)$th subcarrier, $d(k)$ is the data symbol modulated on the kth subcarrier, N is the size of FFT and IFFT, N_1 and N_2 are the indexes of the left- and rightmost subcarriers of the signal spectrum with $N_1 \leqq 0$ and $N_2 > 0$. If the reserved gap width N_{gap} is not smaller than the sideband BW, i.e., $N_{\text{gap}} \geq |N_1 - N_2|$, the signal by definition belongs to the typical gapped OFDM proposed in [1]and [19]. If the gap width smaller than the sideband BW, $N_{\text{gap}} < |N_1 - N_2|$, the signal then becomes the gapless or gapped VSSB-OFDM, depending on whether the gap width N_{gap} equals zero or not. The signal in (1) has not been transmitted so that there is no degrading factor on it. After transmission, the signal would be distorted by the electrical/optical components and the transmission effects in fiber. We denote the discrete-time frequency responses of the transmitter, fiber CD, optical filters, and receiver as $H_T(k)$, $H_{\text{CD}}(k)$, $H_O(k)$, and $H_R(k)$, respectively. The response $H_O(k)$ considers all the optical filtering effects and can be written as the multiplication of each individual optical filter throughout the link, $H_O(k) = \prod H_{oi}(k)$ with $H_{oi}(k)$ accounting for the response of the ith optical filter in the link. After transmission, the optical signal prior to the photodiode can be written as

$$\begin{aligned} E_t(n) &= H_T(-N_2)H_{\text{CD}}(-N_2)H_O(-N_2)Ae^{j2\pi(-N_2)n/N} \\ &\quad + \sum_{k=N_1}^{N_2} H_T(k)H_{\text{CD}}(k)H_O(k)d(k)e^{j2\pi kn/N} \\ &= H_{\text{TR}}(-N_2)Ae^{j2\pi(-N_2)n/N} + \sum_{k=N_1}^{N_2} H_{\text{TR}}(k)d(k)e^{j2\pi kn/N} \end{aligned} \tag{2}$$

where, for simplicity, we denote the overall transfer function from the transmitter to the photodiode as $H_{\text{TR}}(k)$, that is, $H_{\text{TR}}(k) = H_T(k)H_{\text{CD}}(k)H_O(k)$. After the photodiode, which we model as a simple square-law detector, the converted electrical signal can be expressed as

$$\begin{aligned} I_c(n) &= |E_t(n)|^2 \\ &= |H_{\text{TR}}(-N_2)A|^2 \\ &\quad + 2\text{Re}\left\{ H^*_{\text{TR}}(-N_2)A^* \right. \\ &\quad \left. \times \sum_{k=N_1}^{N_2} H_{\text{TR}}(k)d(k)e^{j2\pi(k+N_2)n/N} \right\} \\ &\quad + \left| \sum_{k=N_1}^{N_2} H_{\text{TR}}(k)d(k)e^{j2\pi kn/N} \right|^2 \end{aligned} \tag{3}$$

where * represents the complex conjugator and $\text{Re}\{x\}$ takes the real value of x. The first term of (3) is the dc, the second term represents the desired signal, and the third one is the beat interference, SSBI. The relative power between the desired signal and the SSBI can be controlled by manipulating the CSPR value at the transmitter. For instance, with a smaller CSPR, meaning that $|A|^2/\sum|d(k)|^2 \ll 1$, the SSBI interference is relatively large with respect to the desired signal and thus the system dominantly suffers from the SSBI interference. While with a larger CSPR, that is $|A|^2/\sum|d(k)|^2 \gg 1$, the desired signal becomes relatively large compared with SSBI and the system

performance would be mainly limited by the noises and other transmission distortions.

To prevent the high-frequency noise, distortions, and the residual images from aliasing into the signal band due to the limited sampling rate of ADC, a post electrical filter, also referred to as the antialiasing filter, with a BW smaller than the Nyquist frequency of ADC would be necessary before the signal being sampled by ADC. We denote the frequency response of the receiver as $H_R(k)$, which considers the cascaded responses of the photodiode, antialiasing filter, and ADC. The filtered electrical signal can be represented as

$$I_{\text{sig}}(n) = 2\text{Re}\left\{ H^*_{\text{TR}}(-N_2)A^* \times \sum_{k=N_1}^{N_2} H_R(k+N_2)H_{\text{TR}}(k)d(k)e^{j2\pi(k+N_2)n/N} \right\} \quad (4)$$

and the filtered SSBI is expressed as

$$I_{\text{SSBI}}(n) = \sum_{k_2=N_1}^{N_2}\sum_{k_1=N_1}^{N_2} H_R(k_1-k_2) \times H_{\text{TR}}(k_1)H^*_{\text{TR}}(k_2)d(k_1)d^*(k_2)e^{j2\pi(k_1-k_2)n/N}. \quad (5)$$

From (5), we found that the SSBI is distributed over the frequencies from the leftmost subcarrier, $\min\{k_1-k_2\} = N_1 - N_2$, to the rightmost subcarrier, $\max\{k_1-k_2\} = N_2 - N_1$, where $\min\{x\}$ and $\max\{x\}$ take the minimum and maximum values of x. This indicates that the SSBI of the conventional gapped OFDM ($N_{\text{gap}} \geq |N_1 - N_2|$) will entirely fall on the reserved gap without interfering with the desired signal, while the SSBI of the proposed VSSB-OFDM ($N_{\text{gap}} < |N_1 - N_2|$) will fully or partially overlap with the desired signal and the iterative equalizer is thus required to extract the data from SSBI.

III. Iterative Detection

A. Operation Principles

Since the VSSB-OFDM signal is linearly field-modulated in nature, the beat interference SSBI among the data subcarriers at the photodiode will yield a nonnegligible interference to the signal. To mitigate the impacts of SSBI, we introduce an iterative estimation and cancellation technique at the receiver with its operating concept shown in Fig. 3. After the photodiode, the converted interfered signal of one OFDM symbol, $I_m(n) = I_{\text{sig}}(n) + I_{\text{SSBI}}(n)$, is temporarily stored in the memory for the following iterative processes. This interfered signal is first addressed in the same way as the regular OFDM recovering processes, including the FFT, channel equalization, and hard decision. The channel equalization is implemented by reversing the received symbols with the trained channel response, $H_{\text{ch}}(k)$, which by observing (4) is equal to $H_{\text{ch}}(k) = A^* H^*_{\text{TR}}(-N_2)H_R(k+N_2)H_{\text{TR}}(k)$. The decisions of the interfered signal, denoted as $\hat{d}(k)$, are sent to the feedback loop, which consists of the channel deequalizer, IFFT, square-law, and scaling operators for reconstructing the SSBI. The channel deequalizer is used to reload the channel effects onto the decisions of the interfered signal and has the

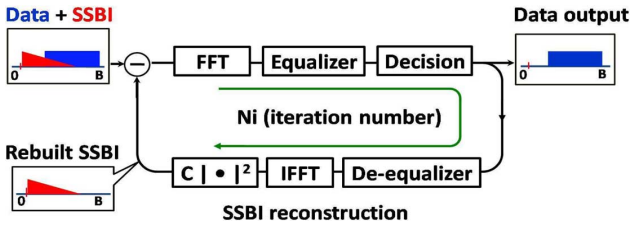

Fig. 3. Iterative estimation and cancellation technique of the VSSB-OFDM. SSBI: signal–signal beat interference; FFT: fast Fourier transform.

output of $H_{\text{ch}}(k)\hat{d}(k)$. After being converted into the time-domain waveform by IFFT, the rebuilt optical signal excluding the optical carrier prior to the photodiode can be written as $\hat{E}_t(n) = \sum_{k=N_1}^{N_2} H_{\text{ch}}(k)\hat{d}(k)e^{j(2\pi kn)/(N)}$. Following the square-law operator that models the photodiode and the scaling operator that resizes the amplitude of the loop output, the rebuilt signal is then yielded as follows:

$$\begin{aligned}\hat{I}_{\text{SSBI}}(n) &= \frac{1}{|H_{\text{TR}}(-N_2)A|^2} \times \left| \sum_{k=N_1}^{N_2} H_{\text{ch}}(k)\hat{d}(k)e^{j2\pi kn/N} \right|^2 \\ &= \sum_{k_2=N_1}^{N_2}\sum_{k_1=N_1}^{N_2} H_{\text{ch}}(k_1)H^*_{\text{ch}}(k_2)\hat{d}(k_1)\hat{d}^*(k_2)e^{j2\pi(k_1-k_2)n/N} \\ &= \sum_{k_2=N_1}^{N_2}\sum_{k_1=N_1}^{N_2} \left[\begin{array}{l} H_R(k_1+N_2)H^*_R(k_2+N_2)H_{\text{TR}}(k_1) \\ \times H^*_{\text{TR}}(k_2)\hat{d}(k_1)\hat{d}^*(k_2)e^{j2\pi(k_1-k_2)n/N} \end{array} \right]. \end{aligned} \quad (6)$$

Since the optical carrier (i.e., the RF tone) is not incorporated in the feedback processing, the output of the square-law operator contains only the SSBI but not the beating term relevant to carrier A.

Compared with the true SSBI expressed in (5), we found the rebuilt SSBI in (6) is only an approximation to the true SSBI in which we assume the receiver has a relatively broader BW with respect to the transmission BW, i.e., $H_R(k) \approx 1$ for k ranges from 0 to $2N_2$. The coefficient, $[1/|H_{\text{TR}}(-N_2)A|^2]$, for scaling the rebuilt SSBI can be obtained with the approach explained in the following section. The rebuilt SSBI in (6) is then used to be subtracted from the stored signal in the memory to obtain a virtually "SSBI-free" signal, i.e., $I_{mi}(n) = I_m(n) - \hat{I}_{\text{SSBI}}(n)$. The resulting signal is then sent into the iteration loop again to initiate the second iteration. Since the SSBI of the newly obtained signal $I_{mi}(n)$ has been virtually removed, the decisions of the second iteration may have fewer error symbols than the first iteration, which, in turn, will yield an improved estimation of SSBI. Thus, with the increased iteration, the interference SSBI could be more accurately estimated and, finally, could be removed with the proposed iterative processes. However, if there are too many error symbols existed in the decision of the initial iteration, the reconstructed SSBI, obtained from the fault decision, would greatly deviate from the true SSBI and causes the iterative process difficult to correct the error symbols in the following iterations, thus the unwanted SSBI might be still retained with

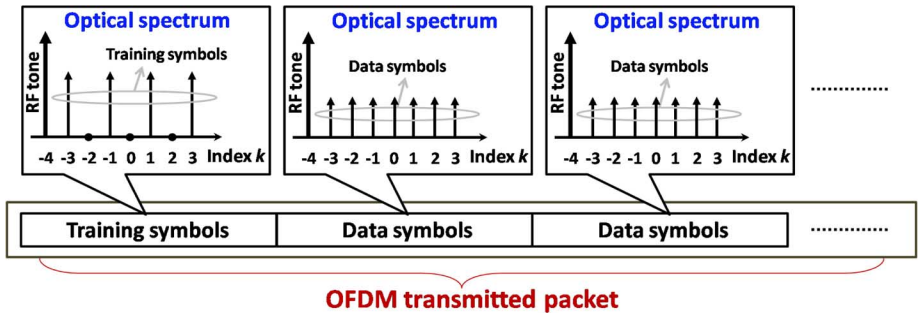

Fig. 4. Optical spectra of the training symbols and the data symbols in a transmitted VSSB-OFDM packet.

the desired signal no matter how many iteration are conducted. There are several impairments, other than the ASE noise, that would result in significant errors in the initial iterations, such as high SSBI and heavy transmission distortions from fiber nonlinearities and PMD. This implies that signals with a smaller gap that yields a relatively large SSBI might not be able to support a longer transmission distance within a given performance margin.

The proposed iterative algorithms are briefly described as follows. With the known channel information of $H_{\rm ch}(k)$, the initially equalized symbol, $R_0(k)$, can be expressed as $R_0(k) = {\rm FFT}[I_m(n)]/H_{\rm ch}(k)$, where ${\rm FFT}[x]$ is the fast Fourier transform of x. We denote the initial decisions of $R_0(k)$ as $d_0(k)$ and start the iterative process with the initial iterative index $i = 0$.

1) Reconstruct the interference SSBI using the decisions, $\hat{d}_i(k)$

$$\hat{I}_{{\rm SSBI},i}(n) = \frac{1}{|H_{\rm TR}(-N_2)A|^2}\left|\sum_{k=N_1}^{N_2} H_{\rm ch}(k)\hat{d}_i(k)e^{j2\pi kn/N}\right|^2. \tag{7}$$

2) Subtract SSBI from the stored signal in the memory and get the new equalized symbols, $R_{i+1}(k)$ as

$$R_{i+1}(k) = \frac{{\rm FFT}[I_m(n) - I_{{\rm SSBI},i}(n)]}{H_{\rm ch}(k)}.$$

3) Make decisions for $R_{i+1}(k)$ and get the new decisions $\hat{d}_{i+1}(k)$ for the $(i+1)$th iteration.
4) Repeat 1)–3) with $i = i + 1$ until the performance converges.

B. Some Practical Designing Issues in Iterative Detector

Before starting the iteration process, we must obtain the channel estimation at the receiver for equalization and de equalization in each iteration loop. However, if the training symbols, used for channel estimation, are transmitted with the same architecture as the regular data symbols, since the iterative equalizer will not function without knowing the channel information, the training symbols will strongly suffer the SSBI and fail to estimate the channel for the data equalization. Thus, a specially designed training symbols as well as the channel estimation for VSSB-OFDM would be needed for a regular operation of the iterative equalizer. There might be several ways to resolve this issue. Here we propose a simple approach that can protect the training symbols from being affected by the SSBI. A suggested transmitted packet for VSSB-OFDM with the training symbol leading ahead is shown in Fig. 4. The training symbols, $t(k)$, are arranged on only the odd-numbered channels while the even-numbered channels are intentionally left blank. The following data symbols, $d(k)$, are modulated on all the channels, as described in Section II. As explained in [4] and [8], the training symbol will not be interfered by SSBI with such a symbol arrangement, i.e., the interleaved OFDM format in [4] and [8], and can be directly used to estimate the channel responses of the odd-numbered channels. As for the even-numbered channels, which are filled with the SSBI after photodiode, their channel responses can be approximated via interpolating the obtained odd-numbered channels' responses. With such an approach, the channel responses of all the channels can be reliably estimated without the SSBI. Notably, to maintain an equalized power transmission in an OFDM packet, the power of the training symbol should be managed as around twice the power of the data symbol, i.e., $\epsilon[|t(k)|^2] = 2\epsilon[|d(k)|^2]$, where $\epsilon[x]$ means the expectation of x, because only half channels are employed.

Although we can obtain the channel response with the interleaved symbols, the rebuilt SSBI in (6) to some extent is still different from the true SSBI in (5). The main difference between (5) and (6) is the location where the receiver response, $H_R(k)$, is applied: for the true SSBI, $H_R(k)$ will be applied for the electrical beat interference after the photodiode, while for the rebuilt SSBI, $H_R(k)$ will be applied for the carrierless optical signal prior to photodiode. Thus, the receiver response in the rebuilt SSBI will have an extra squaring process from the photodiode. However, the true and rebuilt SSBI could be close when the receiver response is almost constant over the down-converted signal band, that is, $H_R(k + N_2) \approx 1$ for $k = 0$ to $2N_2$, then the rebuilt SSBI will have the same form as the real SSBI and can be expressed as

$$\hat{I}_{\rm SSBI}(n) = \left|\sum_{k=N_1}^{N_2} H_{\rm TR}(k)\hat{d}_i(k)e^{j2\pi kn/N}\right|^2. \tag{8}$$

However, if the receiver BW is insufficient to cover the whole signal band, i.e., the amplitude and phase variation of $H_R(k)$ are nonuniform within the signal BW, the rebuilt SSBI would deviate significantly from the true SSBI and cannot give an appropriate estimation, thus resulting in a failure in removing the SSBI. A rigorous approach that can completely separate the desired data and the SSBI is to use the detailed knowledge of the receiver response, $H_R(k)$. However, since the training scheme can only obtain the cascading responses all the way

from the transmitter to the receiver $H_{\rm ch}(k)$, the receiver response alone is difficult to be extracted from this cascading response. A compromised solution to this issue is to load the receiver response $H_R(k)$ into the receiver's signal processor in advance that can help rebuild the SSBI. With the known receiver response $H_R(k)$, the formula of the rebuilt SSBI can be rewritten as

$$\hat{I}_{\rm SSBI}(n) = \frac{1}{|H_{\rm TR}(-N_2)A|^2} \times \sum_{k_2=N_1}^{N_2} \sum_{k_1=N_1}^{N_2} \left[\begin{array}{c} \frac{H_R(k_1-k_2)H_{\rm ch}(k_1)H_{\rm ch}^*(k_2)}{H_R(k_1+N_2)H_R^*(k_2+N_2)} \\ \times \hat{d}_i(k_1)\hat{d}_i^*(k_2)e^{j2\pi(k_1-k_2)n/N} \end{array} \right]. \quad (9)$$

Compared with (6), this rigorous approach requires a more complex algorithm but is with the benefit of accommodating any receiver response. Other drawback relevant to this rigorous approach includes the need for updating the response when aging happens to any component in the receiver.

In addition to the channel estimation, in the first step of the iteration process, the algorithm needs the information of the received carrier power, $1/|H_{\rm TR}(-N_2)A|^2$, as the resizing coefficient to scale the rebuilt SSBI to an appropriate value. This coefficient can be obtained from the received signal at the receiver and is described as follows. If we denote the converted dc current as $I_{\rm dc}$, we can represent this current as $I_{\rm dc} = |H_{\rm TR}(-N_2)A|^2 + \sum |H_{\rm TR}(k)d(k)|^2$. We also assume that the optical filtering has minor influence on the amplitude of the received signal prior the photodiode, that is, $|H_{\rm TR}(-N_2)| \approx |H_{\rm TR}(k)|$ for all k. With such an assumption, the dc current becomes $I_{\rm dc} \approx |H_{\rm TR}(-N_2)|^2(|A|^2 + \sum |d(k)|^2)$, then the carrier power, $|H_{\rm TR}(-N_2)A|^2$, can be expressed as $|H_{\rm TR}(-N_2)A|^2 \approx I_{\rm dc} \times {\rm CSPR}/(1+{\rm CSPR})$, where CSPR is a preselected system parameter known to the receiver. Thus, for a photodiode without an embedded dc block, the dc current can be obtained directly by taking the mean value of the photocurrent. However, if a photodiode is embeded with a built-in dc block, the dc current can still be accessed via $I_{\rm dc} \approx {\rm mean}\{I(t)\} - \min\{I(t)\}$, where ${\rm mean}\{x\}$ and $\min\{x\}$ stand for the mean and minimum values of x, and $I(t)$ is the photocurrent. Note that a normal operation for the iterative detection depends on the negligible optical filtering effect throughout the optical path. Once the signal strongly suffers the optical filtering, the coefficient of $|H_{\rm TR}(-N_2)A|^2$ might be wrongly estimated and the efficiency of the iterative detection will also be diminished.

IV. Experimental Setups

Fig. 5(a) depicts the experimental setup for the gapless and gapped VSSB-OFDM. The OFDM waveform is generated by MATLAB offline in advance and loaded into a two-channel, 10 GS/s arbitrary waveform generator (Tektronix, AWG7102), which functions as a DAC with an amplitude resolution of 8 bits per sample. A total of 144 data channels, along with an additional RF tone, are zero-padded to an IFFT size of $N = 256$.

A cyclic prefix (CP) of $\sim 1/8$ OFDM symbol duration is applied for channel synchronization and for mitigating the intersymbol interference (ISI) caused by fiber CD or the filters' broadening effect in the fiber link. The data rate is operated at 10 Gb/s with a 4-QAM format. The 10 Gb/s data rate can be considered as the raw data rate by ignoring the training symbols due to the negligible training overhead in a direct-detected OFDM system [1]. An optical I/Q modulator, which are made of two parallel differential-phase-shift-keying (DPSK) modulators, is fed with the two outputs of the AWG, which represent the real and imaginary parts of the OFDM signal. The optical output of the I/Q modulator, either gapless or gapped VSSB-OFDM, is then sent into two different transmission architectures, respectively, as shown in the insets (i) and (ii) of Fig. 5(a). For the first transmission scenario (i), the fiber link consists of 5 SSMF spools, and five Erbium-doped fiber amplifiers (EDFAs) with a total transmission length of $\sim$340 km. No optical compensating technique is employed in the fiber link to demonstrate the equalization capability of the VSSB-OFDM signal. The second transmission architecture (ii) contains a recirculating fiber loop, which is constructed with two acoustic-optical (AO) switches, one span of 80 km SSMF, two EDFAs, two optical attenuators, and one optical bandpass filter (OBPF) with a 3-dB BW of $\sim$0.6 nm. The AO switches are used for controlling the transmission distance of the transmitted signal, the first EDFA before the fiber span manipulates the input power to the fiber, the second EDFA and two attenuators in the fiber loop maintain the constant power for each round trip, and the OBPF removes the accumulated out-of-band amplified spontaneous emission (ASE) in the loop. For the receivers in both experimental setups, an optical preamplifier followed by a 0.3-nm OBPF is used before a 12-GHz photodiode, in which a dc block is embedded. The converted photocurrent is sampled and recorded by a real-time scope (Tektronix, TDS6604) with a BW and sampling rate of 6 GHz and 20 GS/s, respectively. The related signal processing, which consists of synchronization, CP removal, FFT, and iterative equalization, are implemented offline in MATLAB for performance evaluation. In both experiments, the channel is estimated with the interleaved training symbols and the SSBI, without the knowledge of the receiver response, is estimated and removed via the formula in (6).

The received back-to-back symbol constellations with and without the iterative equalizer, and the RF spectra of the gapless and gapped VSSB-OFDM are depicted in Fig. 5(b). Without the iterative equalizer, the signal is found to be strongly distorted by SSBI; while with the assistance of the iterative equalizer, most SSBI is removed and the signal quality is found improved. Moreover, a lower SSBI interference and a better signal quality for the gapped VSSB format are also observed. From the RF spectra shown in Fig. 5(b), since the reserved gap bears no data information, the overall signal BW of the gapped VSSB format is $\sim$7.1 GHz, which is broader than $\sim$5.32 GHz of the gapless VSSB format. Since the most significant SSBI congregated in the low frequency region, where is assigned for the frequency gap and bears no data, the burden of the iterative equalizer can be greatly relaxed for the gapped VSSB-OFDM format.

V. Results and Discussions

A. Gapless VSSB-OFD

The measured error vector magnitude (EVM) for the gapless VSSB format as a function of the iteration number with different CSPR values of 2, 6, and 10 dB is shown in Fig. 6. EVM is a measure of signal quality and a lower EVM value

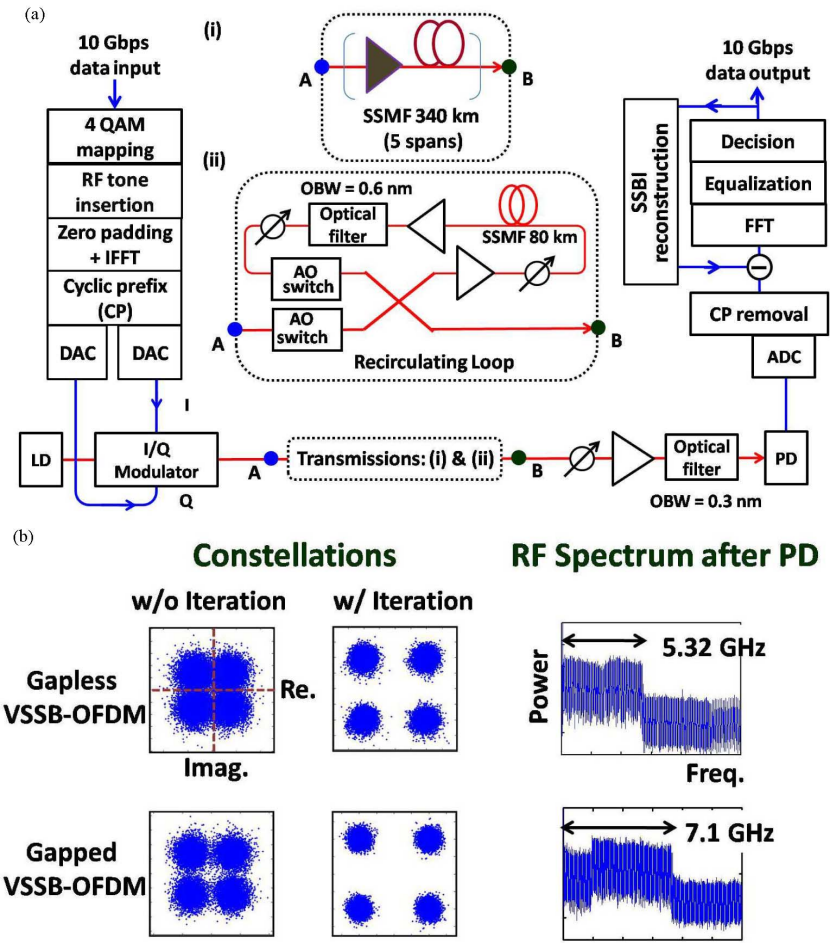

Fig. 5. (a) Experimental setups for the VSSB-OFDM with two different transmission mediums of the (i) cascaded 340-km SSMF and (ii) recirculating fiber loop. (b) Received back-to-back symbol constellations with and without the iteration, and the RF spectra after the photodiode.

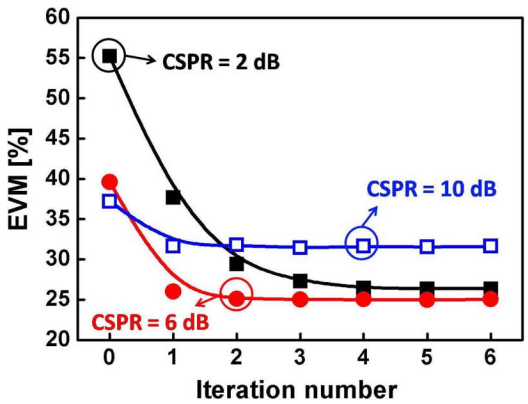

Fig. 6. Measured back-to-back EVM versus the iteration numbers with different CSPR values of 2, 6, and 10 dB.

represents a better system performance. If in detection we consider only the Gaussian noises and ignore the distortions and the other non-Gaussian interferences, an $\mathrm{EVM} = \sim 36\%$ will correspond to a $\mathrm{BER} = 10^{-3}$ for the 4-QAM format [20]. In our experimental demonstrations, the OSNR is fixed at ~18 dB with 0.1 nm resolution for all the EVM measurements unless mentioned otherwise. We found that the performance is better for a larger CSPR when no iterative detection is applied. This can be attributed to the relatively small SSBI for a large CSPR. When the iterative process starts to assist in recovering the received symbols, the system performances move toward a lower EVM for all the three CSPR values. With an increasing iteration (≥ 4), the improvement of the signal quality gradually becomes insignificant and almost disappears when the CSPR is large enough. Since a large number of iteration will increase the computation complexity and a small number of iteration will fail to properly remove the SSBI, an adequate iteration should be applied to balance the computation complexity and system performance. According to the results in Fig. 6, we choose four iterations for the rest measurements since it is the minimum number to stabilize the system performance for the CSPR values ranging from 2 to 10 dB.

Fig. 7 depicts the system performance in terms of EVM as a function of the CSPR. The CSPR of ~4 dB is found to be the optimum value for the system, which indicates that the system is with the best receiving sensitivity. Specifically, this optimum value is different from the previous known results of 0 dB for the gapped OFDM systems [1], [4], [8]. This disagreement can be explained as follows. In the previous DDO-OFDM results, the optimum CSPR of 0 dB is derived under the conditions that after the photodiode the desired signal and the interference SSBI

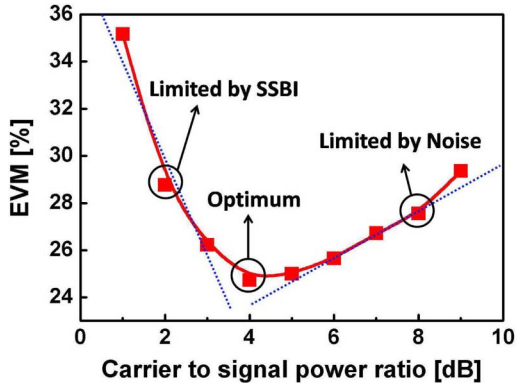

Fig. 7. Measured back-to-back EVM versus the CSPR.

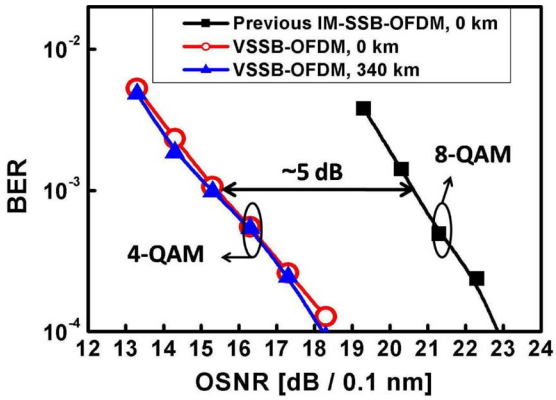

Fig. 8. Measured BER versus the OSNR (0.1 nm) for the previous IM-SSB-OFDM and the proposed gapless VSSB-OFDM. The higher QAM for IM-SSB-OFDM format results from the insufficient sampling rate of AWG.

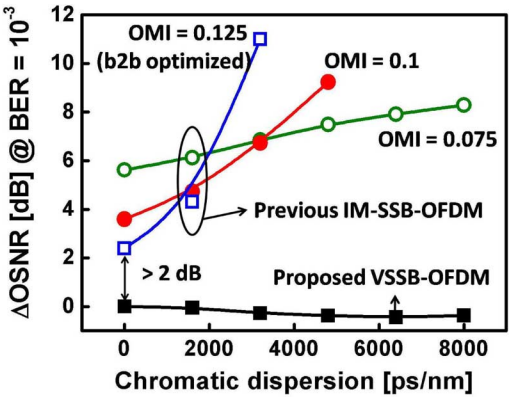

Fig. 9. Simulated results for the previous IM-SSB-OFDM and the proposed gapless VSSB-OFDM.

are deliberately allocated at different frequency bands that can be achieved by reserving a frequency gap or utilizing the interleaved blank subcarriers beforehand [4], [8]. However, the condition has been changed when the desired signal are overlapped with SSBI after photodiode, which is exactly the case of the VSSB-OFDM. To the right of the optimum $\mathrm{CSPR} = 4$ dB, the system performance is limited by the ASE noise, while to the left of $\mathrm{CSPR} = 4$ dB, as has been explained in Section III, due to the involvement of the beat interference SSBI, the system performance degrades rapidly with a decreasing CSPR. It is worth noting that the efficiency of iterative equalizer will determine the power level of the residual SSBI and thus the optimum CSPR is actually a function of the applied iterative algorithm. In other words, to further improve the receiving sensitivity of VSSB-OFDM by employing a lower CSPR value, a better-designed iterative algorithm should be developed.

The bit-error-rate (BER) performance shown in Fig. 8 is measured for both the previous IM-SSB-OFDM and the proposed VSSB-OFDM based on the transmission setup (i) in Fig. 5(a). Due to the higher electrical BW (i.e., the sampling rate of AWG) requirement for the IM-SSB-OFDM, the minimum QAM size, limited by the 10 GS/s AWG, for 10 Gb/s data rate is 8 QAM. The OMIs for both systems are set at ~0.12, which is the optimum value in back-to-back for IM-SSB-OFDM systems. The OSNR at a BER of 10^{-3} for our system is ~5 dB better than that of the previous IM-SSB-OFDM system. This ~5-dB gain could be attributed to: 1) the optimum CSPR, which inherently contributes >2-dB gain in VSSB-OFDM and the details will be discussed later, and 2) the smaller QAM size used in the VSSB-OFDM. Note a smaller QAM size not only has an inherent sensitivity gain but also is more robust to various nonlinearities resulted either from electrical components or optical transmission. Following 340 km uncompensated SSMF, there is negligible penalty observed for VSSB-OFDM.

Fig. 9 compares the CD tolerances between the IM-SSB-OFDM and the proposed VSSB-OFDM by numerical simulations. The simulated data rate and QAM format for the two systems are the same and equal to10 Gb/s and 4 QAM, respectively. For the previous IM-SSB-OFDM, clipping the electrical signal in the transmitter to prevent the high peak-to-average-power ratio (PAPR) has been employed for a better sensitivity [16]. The optimum OMI for the IM-SSB-OFDM is found to be ~0.125, which is limited by the nonlinear transfer function of the MZM. The tradeoff between the sensitivity and the CD tolerance of the IM-SSB-OFDM can be observed in Fig. 9, which shows a larger OMI has a better receiving sensitivity but yields a poor transmission performance, while a small OMI results in a poor sensitivity but experiences a better transmission performance. Compared with the IM-SSB-OFDM, the proposed VSSB-OFDM exhibits an ~2.2-dB OSNR improvement and is much tolerable to the fiber CD.

Note that the proposed iterative detection for VSSB- OFDM is aimed to mitigate the parasitic SSBI after photodiode since the VSSB format modulates the OFDM information onto the optical field rather than the intensity. For the IM-SSB-OFDM, the system performance is mainly limited by the nonlinear distortion of MZM and transmission CD, and thus the proposed iterative detection will not help improve its performance. The CD tolerance of IM-SSB-OFDM could possibly be enhanced via the use of other advanced nonlinear equalizers, for instance, the maximum likelihood sequence equalizer (MLSE) and the decision feedback equalizer (DFE). However, further investigations of these nonlinear equalizers are not within this paper's topic and will not be discussed hereafter.

B. Gapped VSSB-OFDM

In this section, the frequency gap is incorporated to help further improve the performance of VSSB-OFDM system, which

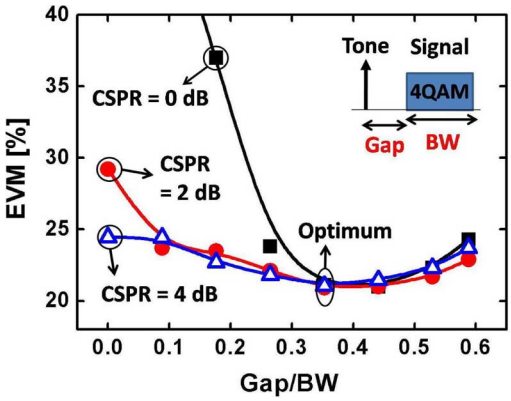

Fig. 10. Measured back-to-back EVM versus the frequency gap for different values of CSPR. The optimum normalized gap is found to be $\eta_{\text{gap}} \approx 0.35$.

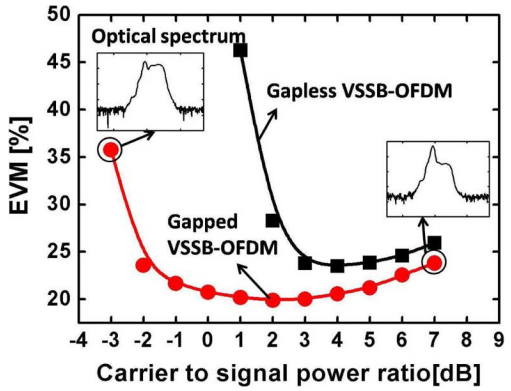

Fig. 11. Measured back-to-back EVM versus the CSPR.

we referred to as the gapped VSSB-OFDM. The EVM performance in back-to-back as a function of the normalized gap width, defined as $\eta_{\text{gap}} = \text{gap}/\text{BW}$, with different values of CSPR is presented in Fig. 10, where $\text{gap} = (N_1 + N_2)$ represents the gap width and $\text{BW} = (N_2 - N_1)$ is the sideband BW. As shown in Fig. 10, for CSPR values of 0, 2, and 4 dB, the optimum gap widths are all found to be $\eta_{\text{gap}} =\sim 0.35$, which trades the SSBI with RIBI, as described in Section II. Notably when the gap width increases, the system performances behave similarly for different CSPR values; however, when the gap width decreases, the system performance is better for a larger CSPR due to relatively smaller SSBI power with respect to the signal power. According to the results shown in Fig. 10, we use the optimum width ratio of $\eta_{\text{gap}} \approx 0.35$ for the gapped VSSB-OFDM in the following measurements.

The EVM as a function of CSPR in back-to-back is shown in Fig. 11. There are several differences between the gapped and gapless VSSB formats. First, the gapped format, with less SSBI, exhibits better sensitivity than the gapless VSSB format over the CSPR values ranging from -3 to 7 dB. Second, the performance difference between the two formats becomes smaller for a lager CSPR, while this difference is enlarged rapidly as CSPR decreases. The reason is that the performance with larger CSPR is mainly limited by ASE noise, to which both formats behave similar robustness, while the performance with lower CSPR is dominantly affected by the SSBI, from which the gapped format suffered less. The third difference is that the gapped format is less

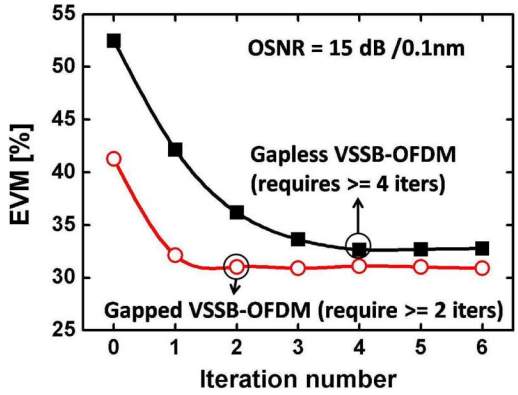

Fig. 12. Measured back-to-back EVM versus the iteration number.

sensitive to CSPR variation around $\text{CSPR} = 0$ dB since SSBI in the gapped format only takes significant effect for smaller values of CSPR (< -2 dB). Because the CSPR of the received signal might vary with the cascaded optical filtering effects in the link, insensitivity of performance to CSPR could avoid the filtering-induced OSNR penalty, thus promising a more reliable transmission quality. The optical spectra for the gapped format with $\text{CSPR} = -3$ and 7 dB are given in the insets showing the higher carrier power for a larger CSPR (i.e., 7 dB).

We also measure the back-to-back EVM as a function of the iteration number at an $\text{OSNR} = 15$ dB for both gapless and gapped VSSB formats in Fig. 12. The required minimum iteration for the gapped VSSB format is found to be $\sim$2 for achieving a steady system performance, while at least four iterations are required for the gapless format. Since each iteration will comprise one FFT and one IFFT computations, the real-time data throughput will be strongly limited if too-many iterations are needed. Thus, the fewer required iterations in the gapped format is apparently an advantage over the gapless format. As the proposed iterative processing only considers a linear transmission, the iterative algorithm would be more complicated if the fiber nonlinearities are taking into account, which is beyond the scope of this paper.

For the result in Fig. 13, the experiments are conducted with the transmission setup (ii) in Fig. 5. In Fig. 13(a), we show the connections between BER performance and OSNR for the gapless and gapped VSSB formats. The CSPR for both formats is fixed at 4 dB, and the iterations applied for the gapless and gapped VSSB formats are 4 and 2, respectively. Meanwhile, the input optical power for each fiber span is controlled at around -7 dBm. The results show that, in back-to-back, the gapped VSSB format has an inherent $\sim$1-dB OSNR advantage over the gapless format due to a reduced SSBI level on the desired signal. After 1600 km uncompensated SSMF transmission, the OSNR penalty for the gapped VSSB format is only 3 dB, while the penalty is over 10 dB for the gapless format. We have considered many possible impairments, such as the laser linewidth [6], PMD effect [23], and fiber nonlinearities [24], which would possibly result in this 8-dB difference. As will be discussed in Fig. 14, both the laser linewidth and the PMD effect will have more serious impacts on the gapped VSSB format and would not contribute this 8-dB penalty, while based on [24], the fiber nonlinearities with 1600 km SSMF would result in an insignificant effect on OFDM signal providing the input power of -7 dBm.

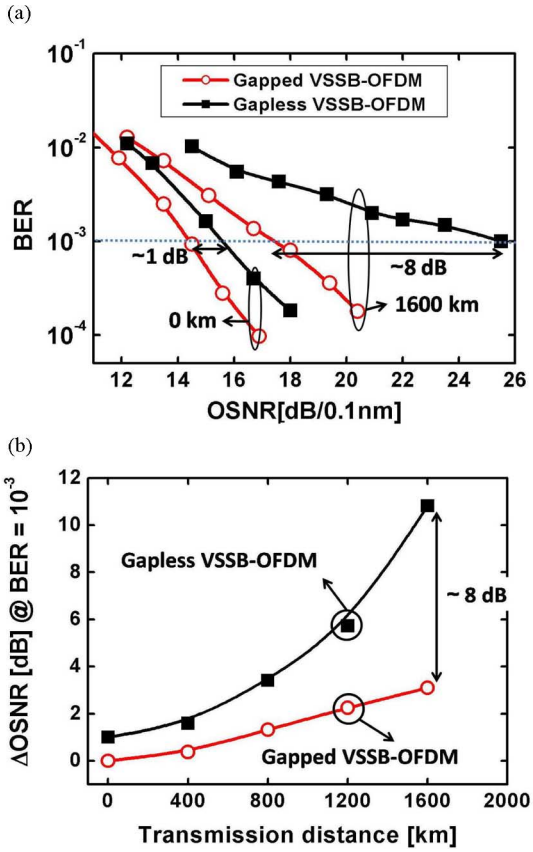

Fig. 13. (a) Measured BER versus the OSNR for the gapless and gapped VSSB-OFDM after 1600 km SSMF transmission. (b) OSNR penalty ($\mathrm{BER} = 10^{-3}$) versus the transmission distance for both formats.

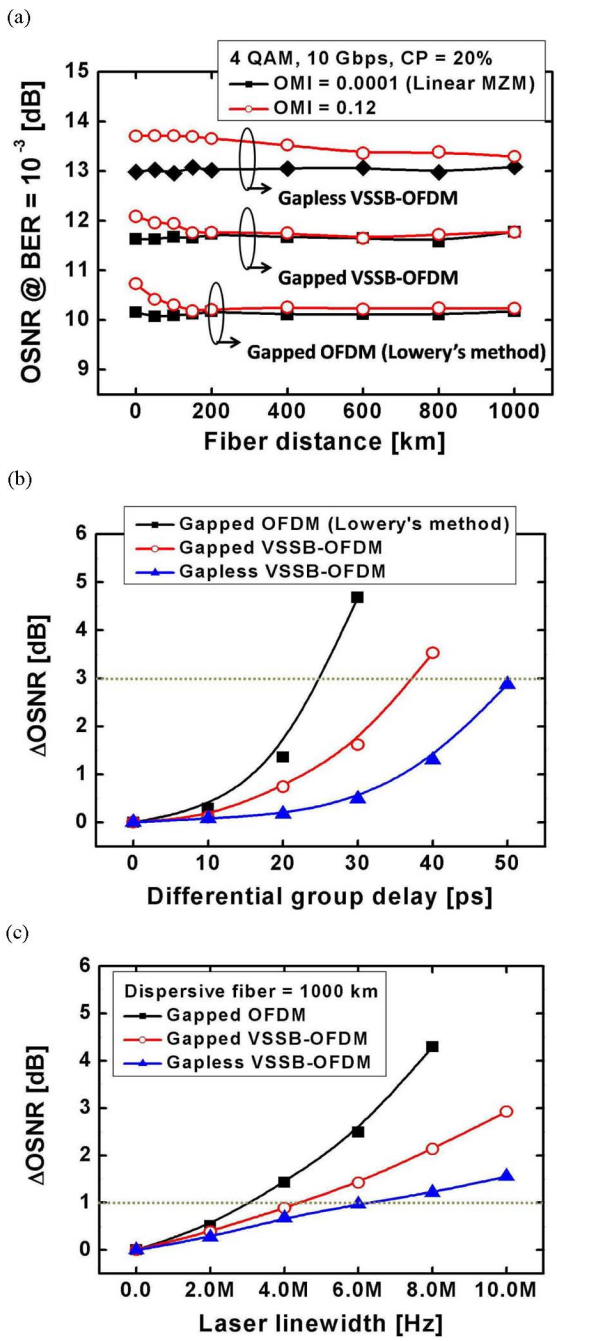

Fig. 14. Numerical results of the gapped OFDM [21], and gapped and gapless VSSB formats. (a) OSNR performance versus fiber distance. The fiber is lossless and linearly dispersive with a dispersion parameter of $D = 16$ ps/(nm·km), (b) OSNR penalty versus DGD, (c) OSNR penalty versus laser linewidth with 1000 km linearly dispersive fiber transmission ($\mathrm{CD} = 16000$ ps/nm).

However, during the loop experiment, we found that the gapless VSSB format is very sensitive to the central wavelength of the laser output while the gapped VSSB format is far more robust to this wavelength deviation. Thus, based on the results in Fig. 11, we conclude that this ~8-dB OSNR transmission penalty between the two formats comes mainly from the cascading filtering effect, which might introduce a low received CSPR that makes the gapless VSSB system more difficult to recover the distorted signal. The OSNR penalty, with respect to the back-to-back performance of the gapped VSSB format, at a $\mathrm{BER} = 10^{-3}$ along the transmission link is presented in Fig. 13(b). The gapless format has an rapid OSNR degradation with the transmission distance in contrast to the gapped format that exhibits a slower raise in the OSNR penalty. The transmission distances with 3-dB OSNR penalty are found to be ~900 and ~1600 km for the gapless and gapped VSSB approaches, respectively. A longer distance, over 1600 km, for the gapped format is achievable but was limited by the experimental structure of our recirculating loop at the time being. The transmission performance for both formats can be further improved if the channel equalizer and de-equalizer of the iterative equalizer have taken all the effects of fiber nonlinearities, PMD, and optical filtering effects into account.

With numerical simulations, we further compare the transmission performances between our VSSB-OFDM approaches and the gapped OFDM [21], which was the first proposal modulating the OFDM signal onto the optical field and utilizing the frequency gap, equal to the sideband BW, to fully avoid the SSBI. In simulations, 4-QAM, 10-Gb/s OFDM systems are considered with the data and total subcarrier numbers of 72 and 256, respectively. The adopted CP is ~20%. The output signal BWs of the gapped OFDM, gapped and gapless VSSB formats are ~12.5, 8.5 and 6.3 GHz, respectively, and the optimum BWs of the utilized optical filters are ~15, 10, 8 GHz, respectively, and the utilized optimum optical BWs are ~15, 10, 8 GHz, respectively. The required OSNR for $\mathrm{BER} = 10^{-3}$ versus the transmission distance are shown in Fig. 14(a). The numerical fiber

for Fig. 14 is linearly dispersive with a dispersion parameter of $D = 16$ ps/(nm·km). First, we use $\mathrm{OMI} = 0.0001$ to ignore the nonlinear distortions in MZM. The gapped OFDM has ∼1 and 3 dB OSNR gains over the gapped and gapless VSSB formats. The reasons are that: 1) the larger gap width would have the signal suffering less SSBI, and 2) would have the signal a higher electrical SNR according to the colored distribution of the electrical beat noise [22], [23]. All the three formats are found to be similarly tolerable to the fiber CD. Later, we use a more practical OMI value of 0.12 and found that for all systems there are ∼0.5 dB OSNR penalties in back-to-back. Interestingly, these penalties are found to be decreased with the accumulated CD due to the coherency reduction among the MZM-induced nonlinear subcarriers after transmission.

In Fig. 14(b), we show the first—order PMD tolerances in terms of the differential group delay (DGD). The nonlinearity of MZM is not considered for Fig. 14(b) and (c). The tolerable DGD with a 3-dB penalty are found to be 25, 36, and 50 ps, respectively, for the gapped OFDM, gapped VSSB, and gapless VSSB formats. Since the PMD-induced fading will strongly attenuate the electrical SNR for those subcarriers far from the optical carrier [23], the narrow BW nature of the VSSB formats will inherently have a better PMD tolerance. Furthermore, we compare their tolerances against the laser linewidth with a fiber distance of 1000 km in Fig. 14(c). We found that a smaller gap format, i.e., the VSSB formats, is more robust to the laser linewidth. The reason is that the linewidth impairment comes from the incoherency between the carrier and sideband, which, when given a fixed amount of CD, would be enlarged with a larger frequency spacing between the carrier and sideband [6].

Although the VSSB formats can increase the SE for DD-OFDM systems, the equalizer involves one FFT and IFFT processing for each iteration to assist reconstruct the SSBI. Compared with the gapped OFDM [1], [19], [21], which needs only one FFT processing, the VSSB formats with N_{i} iterations will have $(N_{\mathrm{i}} + 1)$ FFT and N_{i} IFFT processing, thus yielding an $\sim(2N_{\mathrm{i}} + 1)$ times more complex receiver. Note that the above comparison is mainly based on the FFT and IFFT processing, which are typically considered as the dominant parts in an OFDM transceiver. Hence, an alternate iterative algorithm that uses simpler signal processing would be required with the aim of reaching VSSB's real-time transmission.

VI. Conclusion

We have demonstrated a linearly field-modulated and direct-detected VSSB-OFDM system. Since the beat interference can be iteratively estimated and eliminated via a newly proposed iterative detection, the frequency gap, which typically is reserved for isolating the beating interference, could be removed and the SE can be at most doubly enhanced. We explained in detail how the proposed iterative equalizer functions via the mathematical models in transmission systems, and some possible limitations of this iterative process are also given and discussed. The optimum CSPR for the gapless VSSB format is found to be ∼4 dB and the minimum required iteration with the proposed algorithm is ∼4 to get a steady performance. Compared with the previous intensity-modulated SSB-OFDM, the gapless VSSB-OFDM has been experimentally and theoretically demonstrated with an about 2.2-dB OSNR gain and a much better tolerance to the fiber CD.

To further improve the system performance, we insert an additional frequency gap for the VSSB-OFDM (gapped VSSB-OFDM). With the optimum gapped VSSB format, the signal not only becomes more robust against the variation of CSPR, but also requires fewer iterations that can heavily reduce the processing delay, and thus, increase the data throughput. Besides, the needed power consumption at the receiver associated with the fewer iteration processing could also be abated. The experimental results show that, in addition to a 1-dB OSNR gain in back-to-back, the gapped VSSB format exhibits ∼8-dB OSNR improvement over the gapless format after 1600 uncompensated SSMF transmission using a recirculating loop. To sum up, this spectrally efficient VSSB format, which uses a simple direct up-converted transmitter, saves half the electrical and optical BW, and exhibits a superior system performance both in back-to-back and after long distance transmission. Such an OFDM signal has a great potential as a future-proof format in long-haul transmission.

References

[1] B. J. C. Schmidt, A. J. Lowery, and J. Armstrong, "Experimental demonstrations of electronic dispersion compensation for long-haul transmission using direct-detection optical OFDM," *J. Lightw. Technol.*, vol. 26, no. 1, pp. 196–203, Jan. 2008.

[2] W. Shieh, H. Bao, and Y. Tang, "Coherent optical OFDM: Theory and design," *Opt. Exp.*, vol. 16, pp. 841–859, 2008.

[3] S. L. Jansen, I. Morita, and H. Tanaka, "10 × 121.9-Gb/s PDM-OFDM transmission with 2-b/s/Hz spectral efficiency over 1 000 km of SSMF," presented at the OFC 2008, San Diego, CA, Paper PDP2.

[4] W.-R. Peng, X. Wu, V. R. Arbab, K.-M. Feng, B. Shamee, L. C. Christen, J.-Y. Yang, A. E. Willner, and S. Chi, "Theoretical and experimental investigations of direct-detected RF-tone assisted optical OFDM systems," *J. Lightw. Technol.*, vol. 27, no. 10, pp. 1332–1339, May. 2009.

[5] C. Xie, "PMD insensitive direct-detection optical OFDM systems using self-polarization diversity," in *Proc. OFC 2008*, pp. 1–3, Paper OMM2..

[6] Z. Zan, M. Premaratne, and A. J. Lowery, "Laser RIN and linewidth requirements for direct detection optical OFDM," presented at the CLEO 2008, San Jose, CA, Paper CWN2.

[7] W.-R. Peng, K.-M. Feng, and A. E. Willner, "Direct-detected polarization division multiplexed OFDM systems with self-polarization diversity," in *Proc. LEOS 2008*, pp. 71–72, Paper MH3.

[8] W.-R. Peng, X. Wu, V. R. Arbab, B. Shamee, L. C. Christen, J. Y. Yang, K. M. Feng, A. E. Willner, and S. Chi, "Experimental demonstration of a coherently modulated and directly detected optical OFDM system using an RF-tone insertion," in *Proc. OFC 2008*, pp. 1–3, Paper OMU2.

[9] D. F. Hewitt, "Orthogonal frequency division multiplexing using baseband optical single sideband for simpler adaptive dispersion compensation," in *Proc. OFC 2007*, pp. 1–3, Paper OME7.

[10] W.-R. Peng and S. Chi, "Improving the transmission performance for an externally modulated baseband single sideband OFDM signal using nonlinear post-compensation and differential encoding schemes," presented at the ECOC 2007, Berlin, Germany, Paper P078.

[11] M. Schuster, S. Randel, C. A. Bunge, S. C. J. Lee, F. Breyer, B. Spinnler, and K. Petermann, "Spectrally efficient compatible single-sideband modulation for OFDM transmission with direct detection," *IEEE Photon. Technol. Lett.*, vol. 20, no. 9, pp. 670–672, May 2008.

[12] W.-R. Peng, X. Wu, V. R. Arbab, B. Shamee, J. Y. Yang, L. C. Christen, K. M. Feng, A. E. Willner, and S. Chi, "Experimental demonstration of 340 km SSMF transmission using a virtual single sideband OFDM signal that employs carrier suppressed and iterative detection techniques," in *Proc. OFC 2008*, pp. 1–3, Paper OMU1.

[13] V. Cizek, "Discrete Hilbert transform," *IEEE Trans. Audio Electroacoust.*, vol. AU-8, no. 4, pp. 340–343, Dec. 1970.

[14] R. van Nee and R. Presad, *OFDM for Wireless Multimedia Communications*. Norwood, MA: Artech House, 2000.

[15] J. G. Proakis and D. K. Manolakis, *Digital Signal Processing: Principles, Algorithms, and Applications.*, 4th ed. Englewood Cliffs, NJ: Prentice Hall, 2006.
[16] F. Buchali and F. Supper, "Optimization of an optical OFDM system by peak to average signal ratio reduction," presented at the ECOC 2007, Berlin, Germany, Paper Tu. 5.2.4.
[17] Q. Yang, N. Kaneda, X. Liu, S. Chandrasekhar, W. Shieh, and Y. K. Chen, "Real-time coherent optical OFDM receiver at 2.5-Gbps for receiving a 54 Gbps multi-band signal," in *Proc. OFC 2009*, pp. 1–3, Paper PDPC5.
[18] W.-R. Peng, B. Zhang, X. Wu, K.-M. Feng, A. E. Willner, and S. Chi, "Experimental demonstration of 1600 km SSMF transmission of a generalized direct detection optical virtual SSB-OFDM system," in *Proc. ECOC 2008*, pp. 1–2, Paper Mo3E6.
[19] A. J. Lowery, L. Du, and J. Armstrong, "Orthogonal frequency division multiplexing for adaptive dispersion compensation in long haul WDM systems," in *Proc. OFC 2006*, pp. 1–3, Paper PDP39.
[20] R. A. Shafik, M. S. Rahman, and A. R. Islam, "On the extended relationships among EVM, BER, and SNR as performance metrics," in *Proc. Int. Conf. Electr. Comput. Eng. (ICECE 2006)*, Dec. 2006, pp. 408–411, Dec. 19–21.
[21] B. J. C. Schmidt, A. J. Lowery, and L. B. Du, "Low sampling rate transmitter for direct-detection optical OFDM system," in *Proc. OFC 2009*, pp. 1–2, Paper OWM4.
[22] A. J. Lowery, "Amplified-spontaneous noise limit of optical OFDM lightwave systems," *Opt. Exp.*, vol. 16, pp. 860–865, 2008.
[23] W. R. Peng, K.-M. Feng, A. E. Willner, and S. Chi, "Estimation of the bit error rate for direct-detected OFDM signals with optically pre-amplified receivers," *J. Lightw. Technol.*, vol. 27, no. 10, pp. 1340–1346, May 2009.
[24] A. J. Lowery, L. B. Du, and J. Armstrong, "Performance of optical OFDM in ultra long haul WDM lightwave systems," *J. Lightw. Technol.*, vol. 25, no. 1, pp. 131–138, Jan. 2007.

Wei-Ren Peng photograph and biography not available at the time of publication.

Bo Zhang photograph and biography not available at the time of publication.

Kai-Ming Feng photograph and biography not available at the time of publication.

Xiaoxia Wu photograph and biography not available at the time of publication.

Alan E. Willner (S'87–M'88–SM'93–F'04),photograph and biography not available at the time of publication.

Sien Chi photograph and biography not available at the time of publication.